The Effect of Polyamide End-Group Configuration on Morphology and Toughness of Blends with Maleated Elastomers

A. J. OSHINSKI, H. KESKKULA, and D. R. PAUL*

Department of Chemical Engineering, Center for Polymer Research, University of Texas at Austin, Austin, Texas 78712

SYNOPSIS

The effect of polyamide end-group configuration on morphology generation and toughness of blends with maleated elastomers was investigated. Two difunctional polyamides, a copolymer containing 15% nylon 6,6 and an amine enriched nylon 6, were compared to monofunctional nylon 6 materials of equivalent molecular weight and melt viscosity. Difunctional polyamides have some chains with amine groups on both ends capable of reacting with the maleated rubber phase resulting in crosslinking-type effects. The elastomers used included styrene–butadiene–styrene block copolymers with a hydrogenated midblock, SEBS, and versions with **X**% grafted maleic anhydride, SEBS-*g*-MA-**X**%, and a maleated ethylene/propylene random copolymer, EPR-*g*-MA. Blends based on difunctional polyamides form large, complex rubber particles when compounded in a single-screw extruder; however, by compounding with an appropriate twin-screw extruder, the size and complexity of the particles can be reduced to levels similar to blends with the monofunctional nylon 6 controls. Measurement of the extent of reaction between the amine end groups and the grafted maleic anhydride revealed that a larger number of amine groups are consumed for the difunctional polyamides than for their monofunctional controls. The room-temperature Izod impact strength of blends with the difunctional polyamides is greater than are the corresponding blends with the controls; however, subambient toughness depends mainly on the inherent ductility of the polyamide matrix. © 1996 John Wiley & Sons, Inc.

INTRODUCTION

Previous studies have shown that maleated elastomers form large, complex particles when blended with nylon 6,6 or other nylon *x*, *y* materials in a single-screw extruder compared with the very small, spherical particles formed in blends with most nylon 6 or nylon *x* materials.[1-4] The size and complexity of the rubber particles generated with nylon *x*, *y* materials can, however, be reduced by use of the more intense mixing provided by an appropriate twin-screw extruder.[4] These morphological differences are attributed to the end-group configurations of these polyamides. Nylon *x* materials are usually polymerized in ways that yield chains with only one amine and one acid end group per molecule, i.e., balanced end groups or monofunctional chains. Nylon *x*, *y* materials will contain a distribution of end-group configurations even when there are equal amine and carboxyl end groups; some chains will have one amine and one carboxyl, some will have two carboxyls, while others will have two amine chain ends. Chains with amine groups on both ends are difunctional in the sense that each end can react with the maleated phase leading to the formation of loops or bridges or crosslinking-type effects, whereas, only single-end grafting reactions occur when there is only one amine chain end, i.e., monofunctional, which is typical of most nylon *x* materials.[1,5]

Difunctional polyamides can also be generated in other ways, e.g., formation of nylon *x*/nylon *x*, *y* copolymers[3,6] or incorporation of low molecular weight diamines during polymerization of nylon *x*.[6,7] The purpose of this article was to show that di-

* To whom correspondence should be addressed.

Journal of Applied Polymer Science, Vol. 61, 623–640 (1996)
 CCC 0021-8995/96/040623-18

functional nylons produced in these ways behave similar to nylon *x*, *y*-type materials when blended with maleated elastomers. A nylon 6/nylon 6,6 copolymer containing 15% nylon 6,6 and a nylon 6 terminated with excess amine end groups are compared to monofunctional nylon 6 materials of equivalent molecular weight and melt viscosity in terms of the morphology and properties generated when blended with two types of maleated elastomers.

EXPERIMENTAL

Table I describes the two difunctional polyamide materials and their monofunctional nylon 6 counterparts used as controls. XPN-1539F is a copolymer containing 85% nylon 6 and 15% nylon 6,6 and has a molecular weight and melt viscosity, as determined by Brabender torque rheometry, nearly identical to the unmodified nylon 6 designated as Capron® 8207F. On the basis of the small nylon 6,6 content of the copolymer, the number of chains with two amine ends in XPN-1539F is expected to be much smaller (a factor of 6 to 7 less in the ideal case) than that contained in conventional nylon *x*, *y* materials. The copolyamide has a significantly lower melting temperature, heat of fusion, and tensile modulus[8] than those of the corresponding nylon 6 homopolymer. Therefore, XPN-1539F may be considered more ductile than Capron® 8207F, which may contribute to the toughening results discussed later. XPN-1250 is a nylon 6 that has excess amine end groups caused by the addition of hexamethylene diamine during the polymerization process.[9] The nylon 6 material designated as B2 is used as a control for XPN-1250. Both control materials were made from caprolactam without the addition of other monomers; thus, each chain should have one amine and one acid end group, i.e., monofunctional in the terminology used here.[10,11] However, Table I shows the amine and carboxyl end-group concentrations for the monofunctional nylon 6 materials are actually slightly different from one another. These differences may be attributed to experimental error in the titration procedures or additives that may present.

The two rubber types used in this study are described in Table II. One consists of triblock copolymers having styrene endblocks and a hydrogenated butadiene midblock resembling an ethylene/butene copolymer, designated as SEBS. A series of such materials containing various amounts of maleic anhydride units grafted to the midblock were used, designated here as SEBS-*g*-MA-**X** %, where **X** indicates the nominal content of grafted maleic anhydride (0.5, 1, and 1.84%). The three SEBS-*g*-MA-**X** % elastomers were made from the same nonfunctional precursor (SEBS). The melt viscosity (as indicated by Brabender torque rheometry) decreases in this series as the maleic anhydride content increases, suggesting that some chain scission occurs during maleation.[12] The other rubber is a maleated random ethylene/propylene copolymer, EPR-*g*-MA, grafted with 1.14% maleic anhydride.

Prior to all melt-processing steps, the polyamides were dried in a vacuum oven at 80°C for a minimum of 16 h. The rubbers were dried in a convection oven at 60°C.

Rheological properties of each material were assessed by torque rheometry using a Brabender plasticorder operated at 240°C and 60 rpm with a 50 mL mixing bowl. Torque readings were measured continuously; however, the values reported were taken after 10 min of mixing.

The majority of the blends were prepared using a Killion single-screw extruder ($L/D = 30$, $D = 2.54$ cm) having an intensive mixing head operated at 240°C and 40 rpm. Selected blends were compounded in a Baker-Perkins corotating, fully intermeshing twin-screw extruder ($L/D \sim 15$, $D = 15$ mm) operated at 280°C and 175 rpm.

The degree of maleation in the rubber phase was controlled using combinations of functionalized rubber and its precursor (designated as SEBS/SEBS-*g*-MA-2%) or using the SEBS-*g*-MA-**X** % series of rubbers. All blends were prepared by vigorously dry mixing all the various components together at a ratio of 20% rubber with 80% polyamide prior to feeding to the extruder. The mixture was extruded twice when using the single-screw extruder to ensure adequate mixing. Blends were formed into standard tensile (ASTM D638 Type I) and Izod impact (ASTM D256), 0.318 cm thick, specimens using an Arburg Allrounder injection-molding machine. The ductile–brittle transition temperature was taken as the midpoint of the steplike change in Izod impact strength vs. temperature.

Blend morphology was assessed via transmission electron microscopy (TEM) using ultrathin sections cryogenically microtomed from Izod bars perpendicular to the flow direction. A Reichert-Jung Ultracut E microtome cooled to −45°C and equipped with a diamond knife was used to obtain the ultrathin sections (20–50 nm thick). The sections were exposed to a 2% aqueous solution of phosphotungstic acid for 30 min to stain the polyamide phase. Selected samples were stained using RuO_4 vapors for 15 min. A JEOL 200 CX or a JEOL 1200 EX trans-

Table I Characterization of Polyamide Materials

Supplier's Designation	$\bar{M}_n$[a]	$\bar{M}_n$[b]	[COOH] (μeq/g)	[NH_2] (μeq/g)	Brabender Torque[c] (m − g)	T_m[d] (°C)	ΔH_f[d] (J/gm)	Supplier
Capron XPN-1539F[e]	22,200	19,500	50.1	52.7	655	201	64.1	Allied Signal Inc.
Capron 8207F[f]	22,000	22,000	43.0	47.9	650	219	75.3	Allied Signal Inc.
Capron XPN-1250[g]	18,300	22,300	17.2	72.6	450	222	69.9	Allied Signal Inc.
Ultramid B2[f]	19,400	19,500	48.5	54.0	425	223	69.1	BASF Corp.

[a] From intrinsic viscosity measurements using $[\eta] = 5.26 \times 10^{-4} \bar{M}_w^{0.745}$ assuming that $\bar{M}_n = 1/2\ \bar{M}_w$.
[b] From end-group analysis assuming only NH_2 or COOH groups at chain ends, i.e., $\bar{M}_n = 2/([NH_2] + [COOH])$.
[c] Torque value taken after 10 min of mixing at 240°C and 60 rpm.
[d] From DSC analysis of injection-molded specimens at 10°C/min.
[e] 85/15 nylon 6/66 copolymer.
[f] Nylon 6, not chemically modified.
[g] Nylon 6 with enriched amine chain ends resulting from hexamethylene diamine used in the polymerization.

mission electron microscope operating at 120 kV was used to view the specimens.

Rubber particle-size analysis employed a semiautomatic digital image analysis technique using IMAGE® software developed for the National Institutes of Health. The apparent diameter was determined by scanning TEM photomicrographs and outlining the perimeter of each particle; the average of the longest dimension and the dimension perpendicular to the major axis were defined as the particle size. Typically, over 200 particles and several fields of view were analyzed. Because of the nonspherical nature of the particles, no corrections were applied to convert apparent particle diameters to true particle sizes[13–15]; the methods described in the literature are not applicable for complex shapes. From image analysis, number, weight, and volume-average diameters were calculated from the following relationships:

$$\bar{d}_n = \sum n_i d_i \Big/ \sum n_i \quad (1)$$

$$\bar{d}_w = \sum n_i d_i^2 \Big/ \sum n_i d_i \quad (2)$$

$$\bar{d}_v = \sum n_i d_i^4 \Big/ \sum n_i d_i^3 \quad (3)$$

where n_i is the number of rubber particles within the diameter range i.[14,16–18]

The acid and amine end-group concentrations for each nylon 6 material and certain blends were de-

Table II Rubbers Used in This Study

Designation Used Here	Material (Supplier's Designation)	Composition	Molecular Weight	Brabender Torque[a] (m − g)	Supplier
SEBS	Kraton G 1652	29% wt styrene	Styrene block = 7,000 EB block = 37,500	1050	Shell Chemical Co.
SEBS-*g*-MA-0.5%	Kraton RP-6510	29% wt styrene 0.46% wt MA[b]	N/A	980	Shell Chemical Co.
SEBS-*g*-MA-1%	Kraton FG-1921X	29% wt styrene 0.96% wt MA[b]	N/A	815	Shell Chemical Co.
SEBS-*g*-MA-2%	Kraton FG-1901X	29% wt styrene 1.84% wt MA[b]	N/A	650	Shell Chemical Co.
EPR-*g*-MA	Exxelor 1803	43% wt ethylene 53% wt propylene 1.14% wt MA[b]	N/A	995	Exxon Chemical Co.

[a] Brabender torque taken after 10 min of mixing at 240°C and 60 rpm.
[b] Determined by elemental analysis after solvent/nonsolvent purification.

termined using titration methods.[6,19–26] The acid concentration was analyzed by dissolving the polyamide in benzyl alcohol at 110°C and titrating the hot solution to a phenolphthalein end point with 0.01*N* KOH/benzyl alcohol. The amine concentration was determined by poteniometric titration, first by dissolving the polyamide in a 15/85 methanol/phenol solution for 48 h and determining the pH inflection point while adding a 0.01*N* perchloric acid/methanol solution. Blends of nylon 6 and rubber were analyzed for residual amine concentration as a means of determining the extent of reaction, assuming that the dominate reaction is between amine end groups and anhydride units to form imide linkages.[27,28] Izod bars of the blends were cut into small pieces (0.5 × 0.5 cm), dried for 24 h at 60°C, and dissolved in a 15/85 methanol/phenol solution using high agitation for 48 h. The result is a viscous solution which can then be titrated in the same manner as neat nylon 6 with the exception that additional time must be given for the perchloric acid solution to react and allow the pH reading to stabilize. A more detailed description of the procedure is presented elsewhere.[8] Intrinsic viscosities were determined by a 100 mL Cannon-Fenske viscometer at 25°C using dilute solutions (<0.4 g/dL) of polyamide in *m*-cresol.

POLYAMIDE CHARACTERIZATION

The number-average molecular weight of each nylon 6 material was calculated from the results of end-group analysis and from intrinsic viscosity measurements. The correlation between intrinsic viscosity and molecular weight developed by Tuzar and Kratchovil,[29]

$$[\eta] = 5.26 \times 10^{-4} \bar{M}_w^{0.746} \qquad (4)$$

using *m*-cresol as a solvent at 25°C was used in this study. The average molecular weight, $\bar{M}_n$, was calculated by dividing $\bar{M}_w$ from eq. (1) by two; this assumes that each sample has the most probable distribution. If all end groups are either amines or acids, then the following applies:

$$\bar{M}_n = 2/([NH_2] + [COOH]) \qquad (5)$$

The values of $\bar{M}_n$ obtained from this relation are plotted vs. the $\bar{M}_n$ from intrinsic viscosity in Figure 1(a). Additional monofunctional nylon 6 materials are shown for comparison.[30] The experimental data lie close to the theoretical 45° line except for the two difunctional materials. XPN-1250 lies above the line, suggesting that either all the chain ends are not accounted for during the end-group titration procedure or this material was chemically modified in other ways. Table I shows that the two methods used to calculate molecular weight of XPN-1250 differ by nearly 14%. This difference may be attributed to experimental error, other types of chemical modifications, or that eq. (4) does not strictly describe such chemically altered nylon 6 homopolymers. XPN-1539F lies slightly below the theoretical 45° line; however, since eq. (1) was developed for nylon 6 homopolymers values for copolymers may differ slightly.

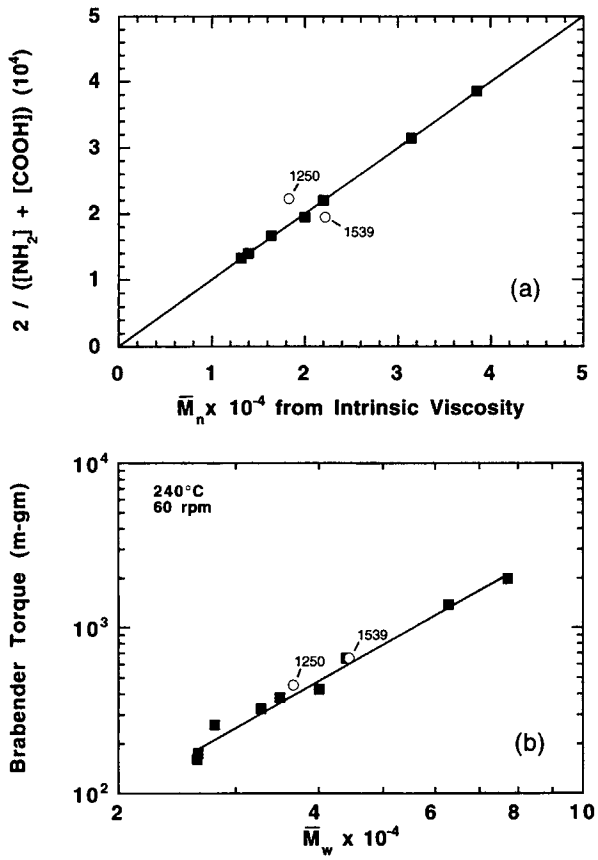

Figure 1 Characterization of polyamides in Table I and nylon 6 materials described elsewhere (8): (a) number-average molecular weight determined by end-group analysis vs. that from intrinsic viscosity (see text for details); (b) melt viscosity of polyamide as indicated by Brabender torque rheometry vs. the weight-average molecular weight determined from intrinsic viscosity measurements. The open circles designate the difunctional polyamides XPN-1250 and XPN-1539F, and the closed squares are monofunctional nylon 6 materials.

The Brabender torque values provide a measure of the melt viscosity for these materials and is plot-

ted vs. the $\bar{M}_w$ from intrinsic viscosity in Figure 1(b). The difunctional nylons fall along the line established by the monofunctional nylon 6 materials. The slope of the line is equal to 2.33, which is less than the value of 3.4, suggesting that the effective shear rate in the Brabender experiment is well above the low shear limit for Newtonian behavior.

EFFECT OF END-GROUP CONFIGURATION ON BLEND MORPHOLOGY

Transmission electron microscopy (TEM) and image analysis techniques were used to determine the effect of the extent of polyamide end-group configuration and the maleic anhydride content of the rubber phase on rubber particle size and distribution. Since the viscosity of the dispersed phase relative to that of the matrix is a critical parameter in morphology generation for both reactive and nonreactive systems,[31-39] the monofunctional control materials were selected based on their melt viscosities, as determined by Brabender torque response, to match those of the difunctional nylons. Therefore, differences in rubber particle size and shape should be the result of the chemical nature of these materials and not rheological issues.

Figure 2 shows TEM photomicrographs for blends of SEBS and the maleated SEBS-*g*-MA-**X** % elastomers with the copolyamide, XPN-1539F, and the amine-terminated nylon 6, XPN-1250. The rubber phase appears as white, nonspherical domains within a dark polyamide matrix with the exception of the blend of SEBS-*g*-MA-2% with XPN-1539F which was stained with RuO_4 where the rubber phase is dark and the matrix is white. When the maleic anhydride content in the rubber phase is less than 1%, the rubber particles are large and semispherical. However, for maleic anhydride contents of 1% or greater, the rubber particles become smaller but are very complex and contain high levels of occluded polyamide; the rubber phase is in the form of strings, loops, and coils. As shown elsewhere,[8,30] the rubber particles for blends based on the nylon 6 control materials progress from large, semispherical particles containing occluded nylon 6 when the maleic anhydride content is low (<1%) to very small, spherically shaped particles with very low amounts of occluded matrix material at high maleic anhydride contents.

Another method of varying the amount of maleic anhydride in the rubber phase is to combine SEBS with SEBS-*g*-MA-2% in various ratios. Previous articles[1,5] have shown that mixing a nonfunctional SEBS with one of high grafted maleic anhydride content produces behavior similar to uniformly grafted materials of the same maleic anhydride content. Figure 3 shows TEM photomicrographs of blends of the difunctional polyamides with SEBS/SEBS-*g*-MA-2% mixtures and the SEBS-*g*-MA-**X** % materials where the maleic anhydride content is either 0.5 or 1%. Increasing the maleic anhydride content reduces the rubber particle size for both types of elastomers, but the rubber particles in the blends based on SEBS/SEBS-*g*-MA-2% mixtures appear to be larger, more complex, and not as well dispersed as those based on the SEBS-*g*-MA-**X** % materials. A quantitative analysis of the rubber particle-size distribution of these blends is shown in Figure 4 using cumulative distribution plots. For both difunctional polyamides, the rubber particles are larger in the case of SEBS/SEBS-*g*-MA-2% mixtures, but the distribution of sizes are very similar and appear to be unimodal in both SEBS rubber systems. Cumulative distribution plots for the monofunctional controls indicate that SEBS-*g*-MA-**X** %-type materials generate somewhat smaller particles that are more narrow in size distribution than do the mixtures with SEBS.[8,30]

Blends based on EPR-*g*-MA with either the monofunctional or difunctional polyamides result in morphologies with complex shapes and high amounts of occluded matrix material.[8,30] It was proposed earlier that the morphology of blends with EPR-*g*-MA and SEBS-type elastomers are different due to the lower reactivity, higher melt elasticity of EPR-*g*-MA, and possibly other factors also caused by the structural differences between these rubbers.[30]

The weight-average rubber particle sizes for blends of the various SEBS-*g*-MA-**X** %, SEBS/SEBS-*g*-MA-2%, and EPR-*g*-MA rubber systems with all the polyamides from Table I are plotted in Figure 5 vs. the degree of maleation. For each polyamide material, rubber particle size decreases as the maleic anhydride content increases; however, the particles in blends based on the nylon 6 control materials are approximately one order of magnitude smaller than those for blends with the copolyamide or the nylon 6 with excess amine end groups. The rubber particle size for blends based on SEBS-*g*-MA-0.5% and SEBS-*g*-MA-1% with the difunctional polyamides lie below the line established by the SEBS/SEBS-*g*-MA-2% mixtures, whereas similar blends with the monofunctional polyamide controls show no difference between the two SEBS rubber systems. For both polyamide types, blends

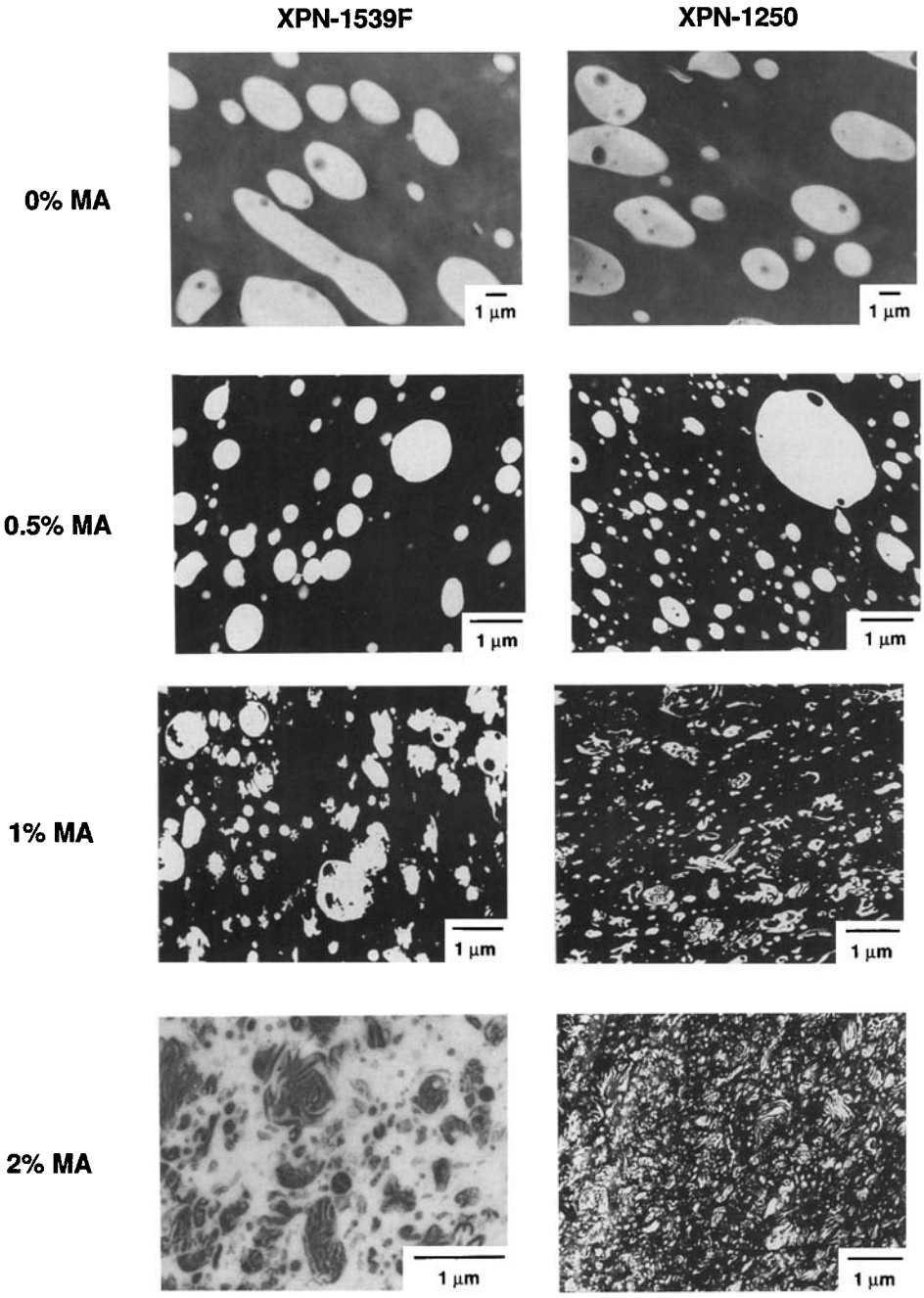

Figure 2 TEM photomicrographs of 20% SEBS-*g*-MA-**X**%/80% polyamide blends as a function of the content of maleic anhydride (**X**) and difunctional polyamide type: **X** = 0. 0.5, 1, and 2%. The polyamide phase is stained dark with phosphotungstic acid for **X** = 0.5 and 1%, and the rubber phase is stained with RuO_4 XPN-1539F blended with **X** = 2%.

based on EPR-*g*-MA have larger rubber particle sizes than do the SEBS-type elastomers.[8] Measures of particle-size polydispersity, $\bar{d}_w/\bar{d}_n$ and $\bar{d}_v/\bar{d}_n$, are shown in Figure 6 vs. the maleic anhydride content for the SEBS-type elastomers. These ratios, represented by the open and closed symbols, steadily decrease as the maleic anhydride content of the rubber phase increases. For a given maleic anhydride content, the polydispersity of rubber particle size for blends based on difunctional polyamides is greater than for blends based on the monofunctional controls.

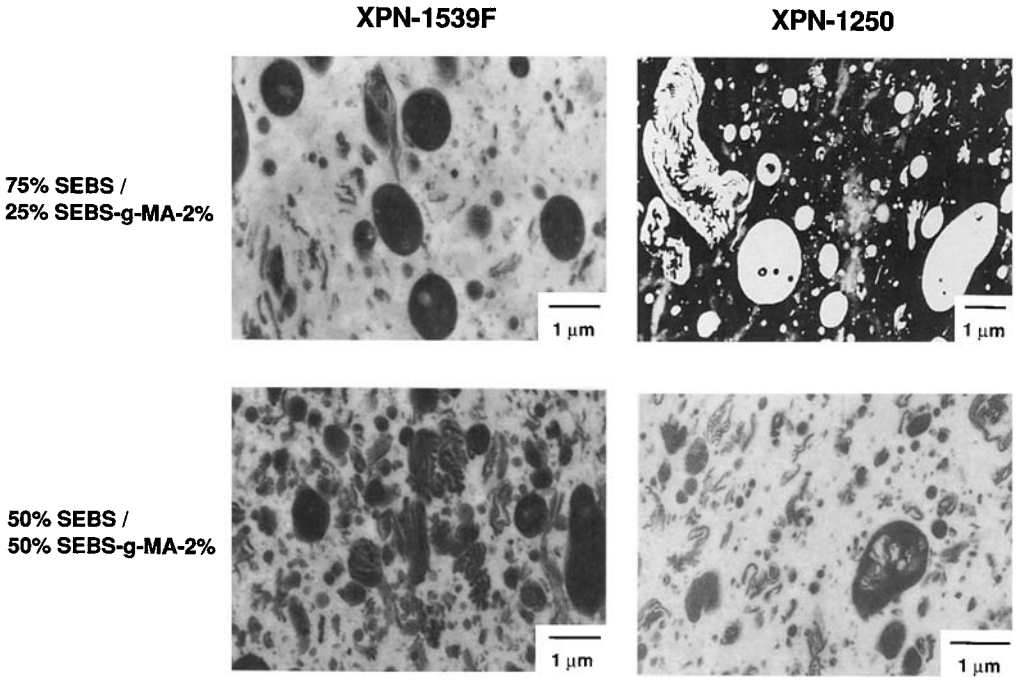

Figure 3 TEM photomicrographs of 20% SEBS/SEBS-*g*-MA-2% (for 25% and 50% SEBS-*g*-MA-2%) blends with 80% difunctional polyamide. The rubber phase is stained dark with RuO_4 with the exception of XPN-1250 blended with 25% SEBS-*g*-MA where the polyamide phase is stained dark with phosphotungstic acid.

EFFECT OF POLYAMIDE TYPE ON EXTENT OF GRAFT REACTION

From the TEM photomicrographs in Figures 2 and 3 and the quantitative results shown in Figures 5 and 6, it is clear that the blends of difunctional and monofunctional polyamides lead to very different morphologies when compounded in the single-screw extruder. Previous studies have attributed these differences to single-end vs. double-end grafting associated with the two types of end-group configurations. Here, a detailed examination is made of the extent of grafting reaction that occurs when these polyamides are blended with maleated elastomers to assess how end-group differences may contribute to morphology generation. For example, the amine-terminated nylon 6, XPN-1250, has a larger number of amine end groups than does its monofunctional control (72.6 vs. 54.0 μeq/g), which potentially could affect the number of graft reactions with maleic anhydride in addition to the nature of the grafting. Also, XPN-1250 presumably has more chains with two amine end groups than does the copolyamide XPN-1539F which may influence the morphology. While it is difficult to determine differences in crosslinking-type reactions that occur with XPN-1250 or XPN-1539F, it is possible to monitor the amine concentration after blending with the maleated elastomers and, thus, to compare their extent of reaction.

The titration technique outlined earlier was used to determine the number of amine end groups before and after blending each polyamide with EPR-*g*-MA and the three SEBS-*g*-MA-**X** % elastomers. The discussion above assumes that the predominate reaction is between the amine groups and the maleic anhydride in the rubber phase to form imide linkages; however, other reactions may occur which can either produce or consume amine groups.[19,27] Experiments using nylon 6 and low molecular weight anhydrides showed that hydrolysis and condensation reactions can become significant at long mixing times (>10 min)[27]; however, the mixing times used here were short, so these reactions should have little effect on the amine concentration during melt processing.[8,30] On this basis, the loss of amine groups can be directly related to imide linkages formed. Figure 7 shows that in all cases the absolute number of amine groups consumed during blending increases as the maleic anhydride content of the rubber phase increases. The greatest difference between polyamide types is seen at a maleic anhydride content of 1.84% (SEBS-*g*-MA-2%). In each comparison, more amine end groups react with maleic

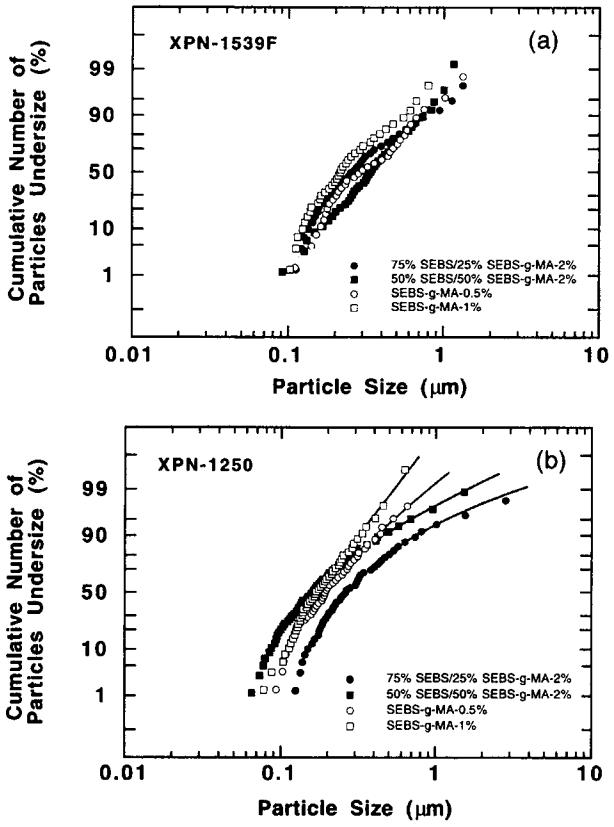

Figure 4 Cumulative apparent particle-size distributions for 20% SEBS-*g*-MA-**X**% (where **X** = 0.5 and 1%) and 20% SEBS/SEBS-*g*-MA-2% (for 25% and 50% SEBS-*g*-MA-2%) blends with 80% difunctional polyamide: (a) XPN-1539F; (b) XPN-1250. The two rubber systems being compared contain approximately 0.5 and 1% maleic anhydride by weight.

anhydride for the difunctional polyamide materials than for their monofunctional controls. For the other SEBS-*g*-MA-**X** % materials (0.5 and 1%), the reaction is nearly complete, i.e., the number of amine groups consumed is approximately equal to the number of maleic anhydride groups available for reaction. There is a large excess of amine groups relative to maleic anhydride groups when the rubber phase contains 0.5 and 1% MA, which evidently leads to a very efficient reaction. However, at MA = 1.84%, the number of amine groups consumed is noticeably less than is the available maleic anhydride content. In this case, the initial number of amine groups for these two polyamides are similar to the initial number of maleic anhydride units.

The failure to achieve complete consumption of the available anhydride units may be influenced by the lack of an excess of amine units to drive the reaction, but one cannot rule out the possibility that to some extent graft reactions may be somewhat self-limiting. As more grafting occurs, it may be difficult for additional chain ends to reach the interface for conformational or rheological (a large increase in melt viscosity accompanies grafting) reasons. In all cases, the amount of amine groups consumed in the blend with SEBS-*g*-MA-2% is somewhat larger for the difunctional polyamides than for the monofunctional controls. The extent of reaction with EPR-*g*-MA with each polyamide is less than expected for an SEBS-*g*-MA material of similar maleic anhydride content. The lower extent of reaction of the EPR-*g*-MA-based elastomer has been observed and discussed previously.[30]

Figure 8 compares the change in amine concentration for blends of SEBS-*g*-MA-2% with various molecular weight monofunctional nylon 6 materials.[30] The absolute number of amine groups that react during blending decreases as the molecular weight increases, but, clearly, blends based on XPN-

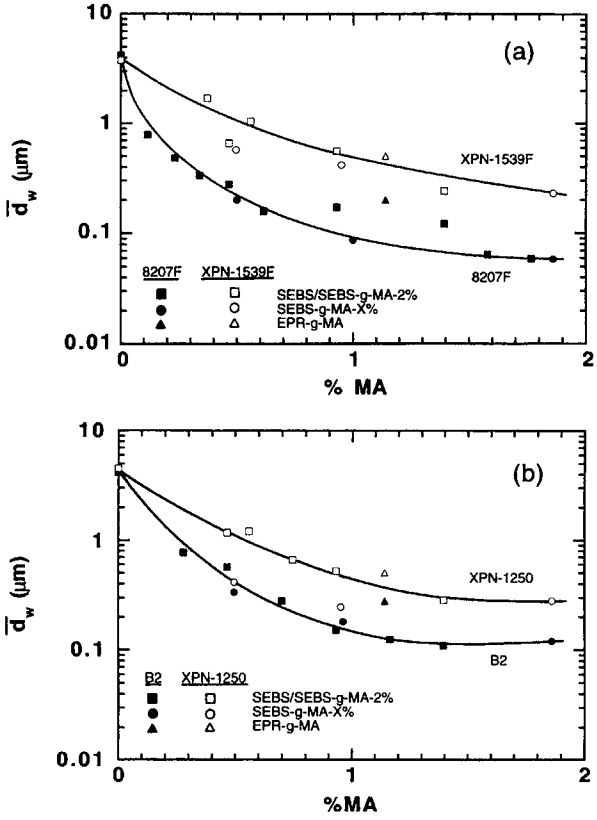

Figure 5 Effect of maleic anhydride content in rubber on weight-average rubber particle diameter for blends of SEBS/SEBS-*g*-MA-2%, SEBS-*g*-MA-**X**%, and EPR-*g*-MA with difunctional and monofunctional polyamides in the ratio of 20% rubber/80% polyamide: (a) XPN-1539F and Capron 8207F; (b) XPN-1250 and B2.

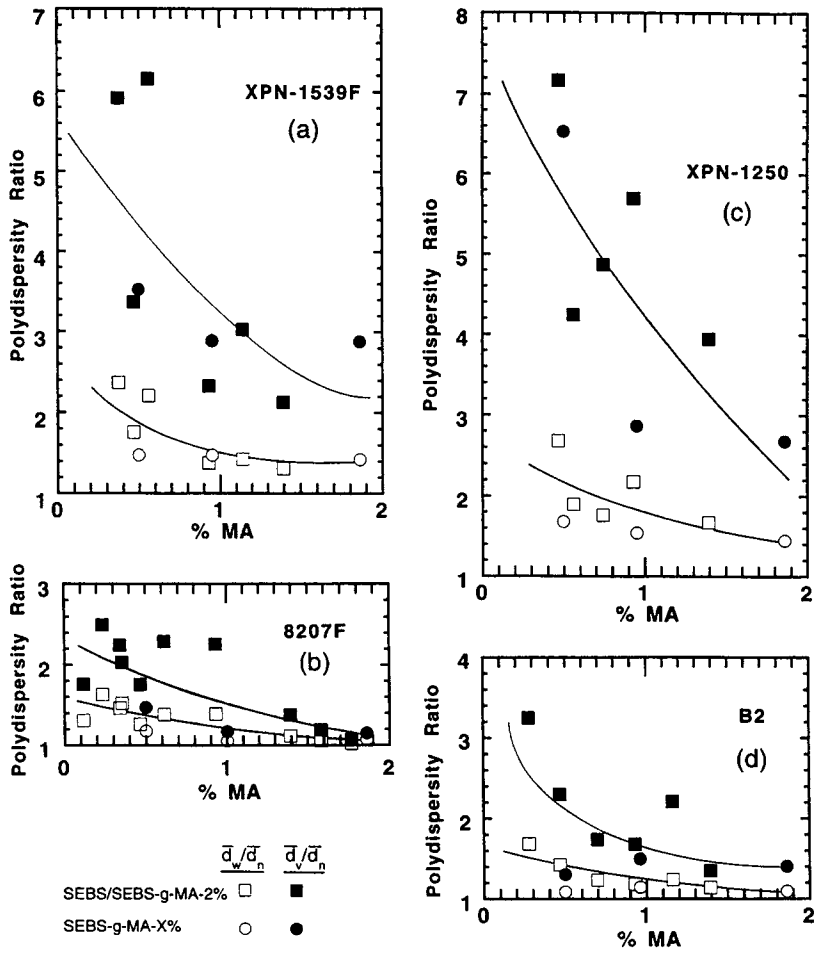

Figure 6 Effect of maleic anhydride content on the polydispersity of rubber particle size for blends of SEBS-*g*-MA-**X**% and SEBS/SEBS-*g*-MA-2% with difunctional and monofunctional polyamides in the ratio of 20% rubber/80% polyamide: (a) XPN-1539F; (b) Capron 8207F; (c) XPN-1250; (d) B2.

1250 and XPN-1539F have larger changes in amine concentration or a greater number of grafting reactions than do corresponding monofunctional nylon 6 materials [see Fig. 8(a)]. However, as shown in Figure 8(b), on a fractional basis, the number of amine end groups reacting is similar for both monofunctional and difunctional polyamides because of the higher initial amine concentration for the difunctional materials. The fraction of amine groups that reacted, or the extent of amine reaction, is defined as

$$\text{Extent of amine reaction} = [NH_2]_o - [NH_2]_b)/[NH_2]_o \times 100 \quad (6)$$

where the subscripts "*o*" refer to the initial amount, and *b*, to the amount after compounding and molding.

Torque rheometry provides useful information regarding the nature of the differences in the grafting reactions exhibited by difunctional nylons vs. monofunctional polyamides.[1,5,40-43] Figure 9 shows Brabender torque responses for blends of the three SEBS-*g*-MA-**X** % elastomers with the polyamides in Table I. Of course, the torque increases with the maleic anhydride content of the rubber phase in all cases. XPN-1539F-based blends have a higher torque during the initial 5 min than those for Capron 8207F. Subsequently, the torque of the blends based on XPN-1593F decreases to similar values as those for Capron 8207F, suggesting that the complex, crosslink structure of the former may be broken down with time. The torques for blends with XPN-1250 are significantly higher than those with its control, B2, for maleic anhydride contents greater than 0.5%. The torques generated for blends based

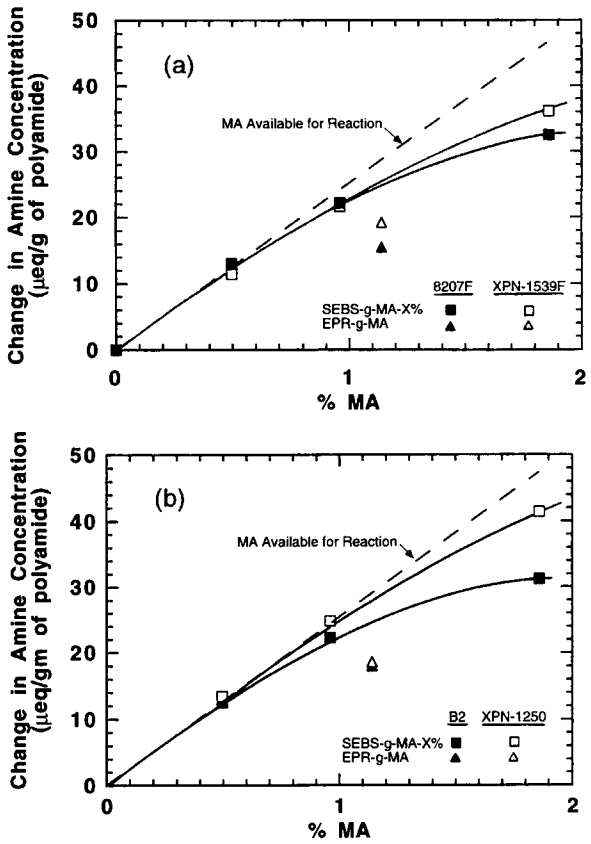

Figure 7 Effect of maleic anhydride content of the rubber phase on the extent of amine reaction in 20% rubber/80% polyamide blends for the rubbers EPR-*g*-MA and SEBS-*g*-MA-X%, following melt compounding and injection molding. The difunctional polyamide and its monofunctional control are compared as follows: (a) XPN-1539F and Capron 8207F; (b) XPN-1250 and B2.

on XPN-1250 are greater than those for XPN-1539F; this implies that the polyamide enriched in amine chain ends, XPN-1250, has a larger fraction of chains with two amine groups than does the copolyamide, XPN-1539F, since in the case of blends based on SEBS-*g*-MA-0.5% and SEBS-*g*-MA-1%, approximately the same number of amine groups reacted for each polyamide. It is interesting to note that the rubber particle size for blends based on the copolyamide, XPN-1539F, with SEBS-*g*-MA-X %, where X = 0.5 and 1%, are twice as large as those for similar blends generated with the polyamide that has been amine-terminated, XPN-1250, but the sizes are nearly identical when X = 2%. One possible explanation is that the higher melt viscosity of the XPN-1250 blends generates more stress on the rubber phase during dispersion, producing smaller rubber particles. As shown later, this relative relationship in rubber particle size between the two difunctional polyamides is maintained even when the blends are compounded in a twin-screw extruder. Regardless, both difunctional polyamides produce blends having rubber particle sizes that are larger than their monofunctional control.

EFFECT OF POLYAMIDE TYPE ON TOUGHNESS

Figure 10 shows the room-temperature Izod impact strength for blends of the polyamides with each rubber system as a function of maleic anhydride content of the rubber phase over the available range. For blends based on SEBS/SEBS-*g*-MA-2% mixtures,

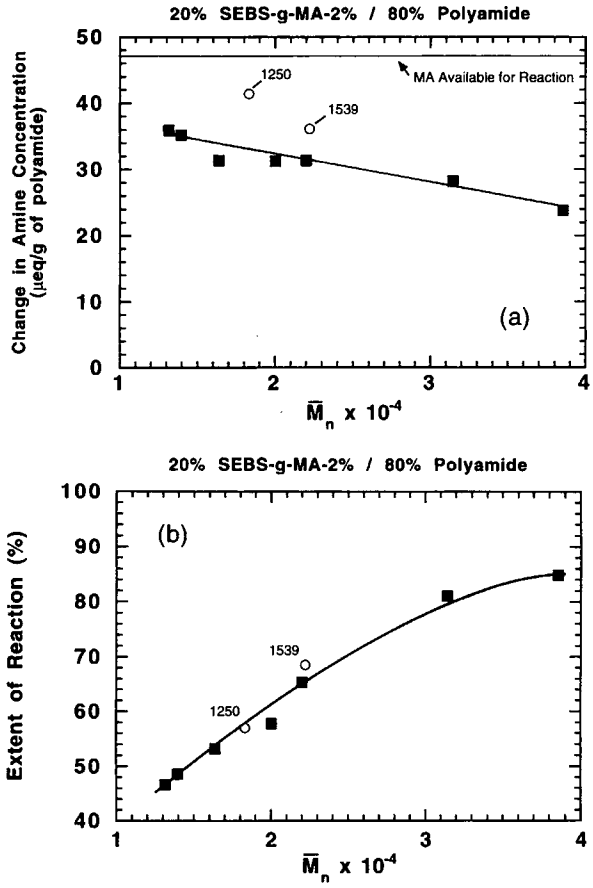

Figure 8 Effect of polyamide molecular weight and type on the amount of amine end groups that react with maleic anhydride in 20% SEBS-*g*-MA-2%/80% polyamide blends, following melt compounding and injection molding, expressed as (a) the change in amine end group concentration as a result of blending and (b) the extent of reaction as defined in eq. (6). The open circles designate the difunctional polyamides, XPN-1250 and XPN-1539F, and the closed squares denote the monofunctional nylon 6 materials.

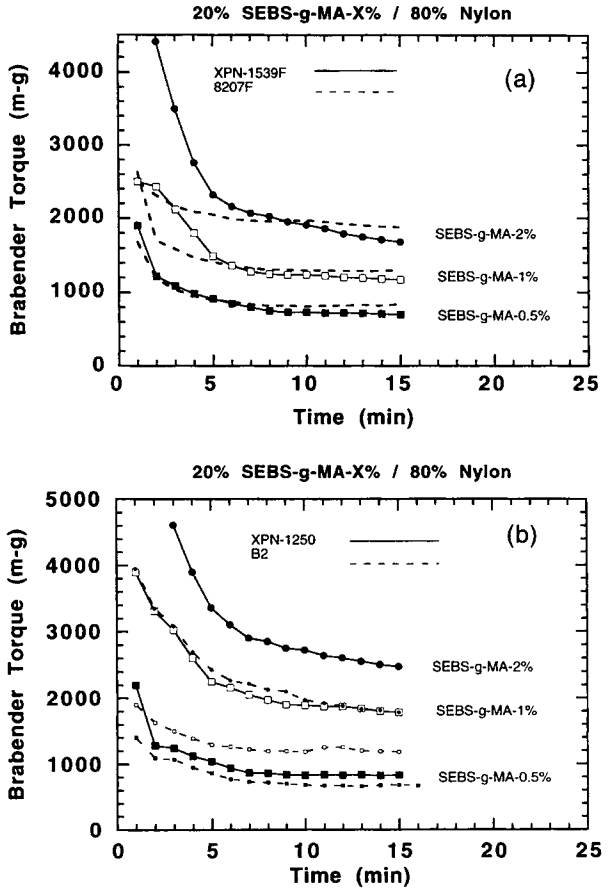

Figure 9 Brabender torque response (at 240°C and 60 rpm) for blends of 20% SEBS-*g*-MA-**X**%/80% polyamide for **X** = 0.5, 1, and 2%. The difunctional polyamide and its monofunctional control are compared as follows: (a) XPN-1539F and Capron 8207F; (b) XPN-1250 and B2.

the difunctional polyamides lead to a plateau impact strength of approximately 1300 J/m at a maleic anhydride content near 1%, whereas for blends with the monofunctional controls, the impact strength reaches a maximum value of approximately 1100 J/m at 0.25% MA and then declines as the level of maleation is increased. For blends based on SEBS-*g*-MA-**X** %-type elastomers (see open circles in Fig. 10), the impact strength for the monofunctional controls fall below the curve established by the blends based on the SEBS/SEBS-*g*-MA-2% mixtures but lie above the curve when compounded with the difunctional polyamides. For blends based on EPR-*g*-MA, the room-temperature Izod impact strength is higher for the difunctional polyamides than for the nylon 6 controls.

Previous studies[4,16,44–47] suggested that rubber particle size or interparticle distance[16,45] are controlling parameters for toughening polyamides. In this study, the weight fraction of rubber has been held constant, making the interparticle distance dependent only on the rubber particle size, as calculated in the usual way.[45] On this basis, the room-temperature Izod impact strength is plotted as a function of the weight-average particle size in Figure 11. Blends based on the SEBS-*g*-MA-**X** % and SEBS/SEBS-*g*-MA-2% rubber systems have identical impact strength when compared at constant rubber particle size when the maleic anhydride content is 1% or greater. However, blends based on SEBS-*g*-MA-0.5% always have a somewhat lower impact strength (see circles below the curves drawn in Fig. 11) than that of SEBS/SEBS-*g*-MA-2% mixtures of an equivalent rubber particle size.[8,48] The blends based on the monofunctional nylon 6 materials show an upper and lower size limit for toughening; however, because rubber particles less than

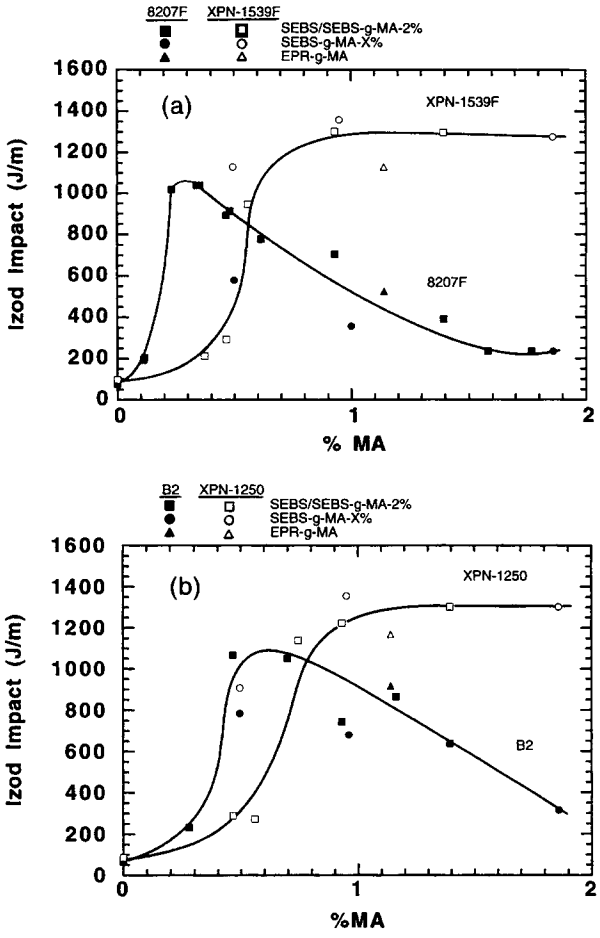

Figure 10 Effect of rubber-phase maleic anhydride content on room-temperature Izod impact strength for blends of EPR-*g*-MA, SEBS-*g*-MA-**X**%, and SEBS/SEBS-*g*-MA-2% with difunctional and monofunctional polyamides in the ratio of 20% rubber/80% polyamide: (a) XPN-1539F and Capron 8207F; (b) XPN-1250 and B2.

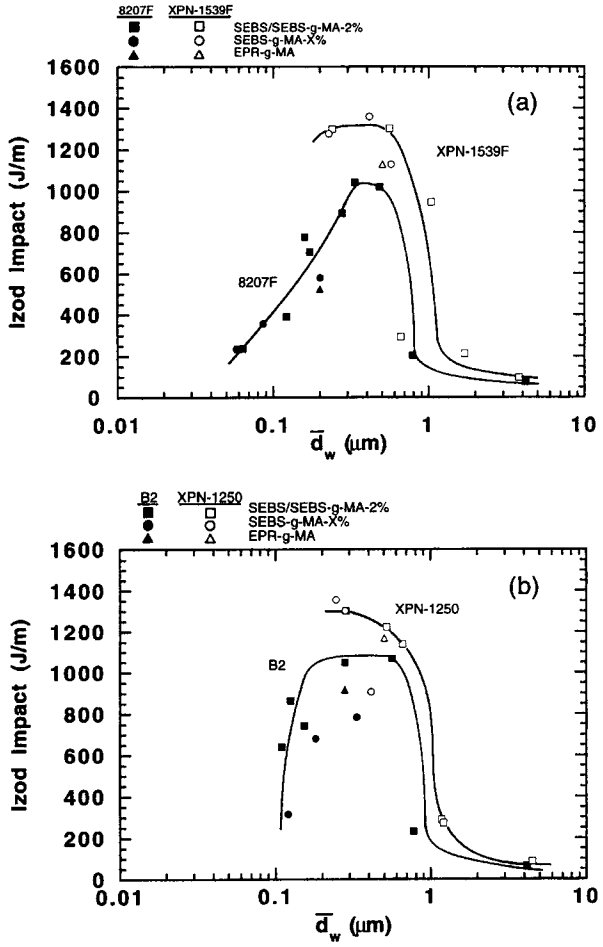

Figure 11 Effect of weight-average rubber particle diameter on room-temperature Izod impact strength for blends of EPR-*g*-MA, SEBS-*g*-MA-**X**%, and SEBS/SEBS-*g*-MA-2% with difunctional and monofunctional polyamides in the ratio of 20% rubber/80% polyamide: (a) XPN-1539F and Capron 8207F; (b) XPN-1250 and B2.

0.2 μm could not be generated with the difunctional polyamides, it was not possible to investigate the lower particle size limit for these materials. In general, blends based on EPR-*g*-MA with the various polyamides in Table I have a lower room-temperature Izod impact strength than do blends with the various SEBS-type elastomers at an equivalent rubber particle size.

The Izod impact strength of these blends was also measured as a function of temperature. Figure 12 shows such plots for blends based on SEBS/SEBS-*g*-MA-2% with the following rubber-phase compositions: 0, 25, 50, 75, and 100% SEBS-*g*-MA-2%; data for other compositions and rubber types can be found elsewhere.[8] In general, Figure 12 shows that blends based on the difunctional polyamides have a higher Izod impact strength above the ductile–brittle transition temperature than those based on the monofunctional controls. Below the ductile–brittle transition temperature, the impact strength is relatively constant regardless of polyamide type.

Ductile–brittle transition temperatures, as defined earlier, deduced from plots like those in Figure 12 are shown in Figure 13 as a function of the maleic anhydride content of the rubber phase. For blends based on either SEBS-*g*-MA-**X** % or SEBS/SEBS-*g*-MA-2% mixtures, the ductile–brittle transition temperature monotonically decreases with increasing maleic anhydride content of the rubber phase and eventually reaches a plateau region that is dependent on the polyamide type. The amount of maleic anhydride required to reach the plateau for blends with the difunctional polyamides is three times greater than that for the monofunctional controls. For Capron 8207F, the ductile–brittle transition temperature goes through a narrow plateau region and then increases when the maleic anhydride content exceeds about 1.5%. As shown previously,[49] the ductile–brittle transition temperatures for blends based on SEBS-type rubbers are restricted to a lower limit of −20°C due to their mechanical properties at low temperatures. However, blends of EPR-*g*-MA with the monofunctional polyamide controls attain ductile–brittle transition temperatures as low as −35°C, whereas blends based on the difunctional polyamides never achieve values below −20°C when compounded in a single-screw extruder.

The ductile–brittle transition data from Figure 13 are replotted as a function of the weight-average rubber particle size in Figure 14. For blends of the monofunctional nylon 6 materials with the SEBS rubber systems, the ductile–brittle transition temperature decreases as the weight-average rubber particle size decreases and reaches a plateau.[8,49] However, for blends based on Capron 8207F, there is a sharp increase in the ductile–brittle transition temperature when the rubber particle size is less than 0.1 μm.[49] For blends based on the difunctional polyamides, the ductile–brittle transition temperature shows a monotonic decrease with little or no indication of a plateau region. On the basis of previous studies using SEBS rubber systems,[49] one would also expect a plateau region to occur for blends with the copolyamide and amine-terminated nylon 6 if the rubber particle size could be reduced below 0.2 μm. It is significant to note that the ductile–brittle transition temperatures for blends based on XPN-1539F are always less than those formed from Capron 8207F at the same rubber particle size, suggesting that the former may be inherently tougher than the latter. The copolyamide has a lower degree

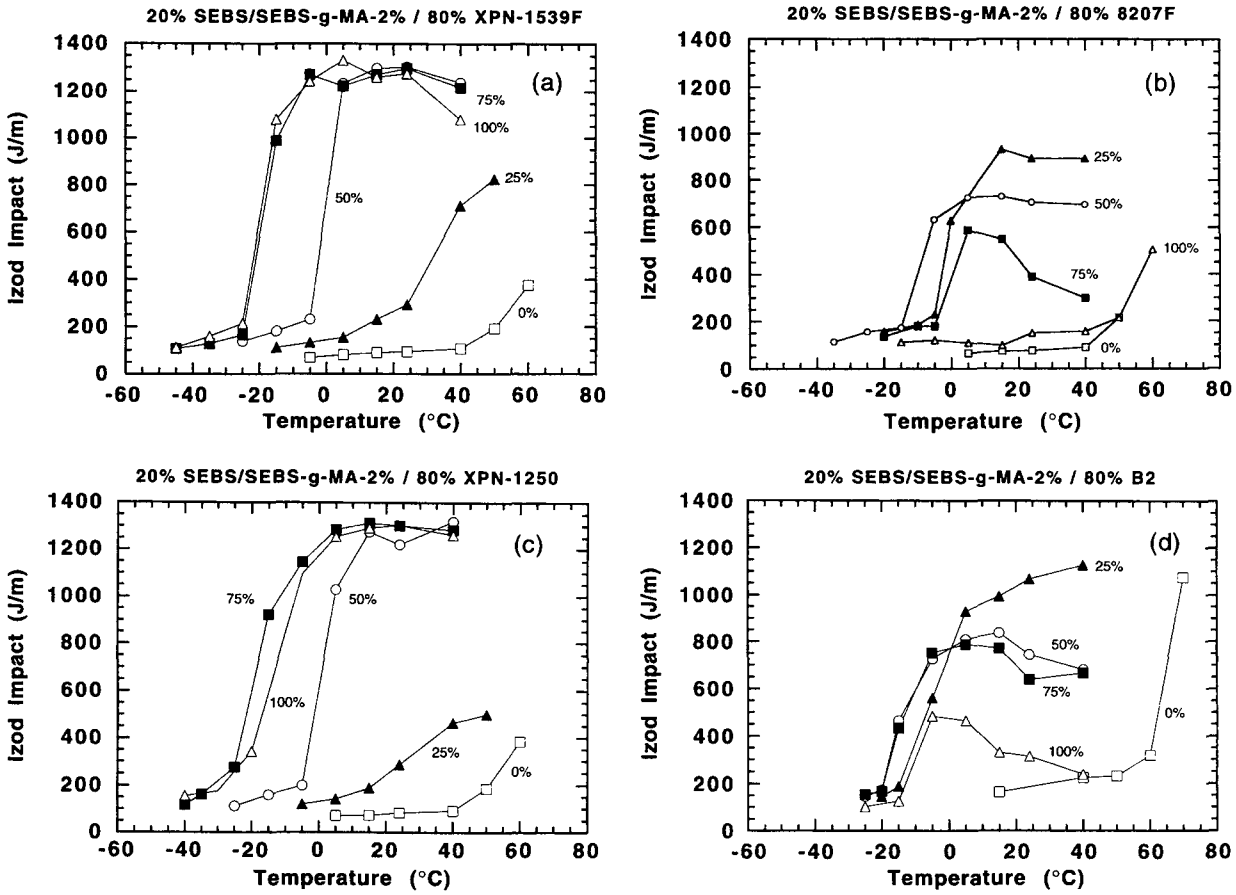

Figure 12 Effect of rubber-phase maleic anhydride content on Izod impact strength vs. temperature for blends of SEBS/SEBS-*g*-MA-2% with difunctional and monofunctional polyamides in the ratio of 20% rubber/80% polyamide where the SEBS-*g*-MA-2% percentage of the rubber phase is varied: (a) XPN-1539F; (b) Capron 8207F; (c) XPN-1250; (d) B2. Data are shown here only for selected mixtures; more complete data are available elsewhere.[8]

of crystallinity and tensile modulus than those of Capron 8207F, which, based on certain criteria for toughening polyamides,[50-55] suggests that the copolymer should be easier to toughen. Comparing XPN-1250 with B2, the ductile–brittle transition temperature is lower for blends with XPN-1250 only when the rubber particle size is less than 0.3 μm. Each of the polyamides in Table I lead to significantly lower ductile–brittle transition temperatures when blended with EPR-*g*-MA then when blended with SEBS-type rubbers at an equivalent rubber particle size.

EFFECT OF EXTRUDER TYPE ON BLEND MORPHOLOGY AND TOUGHNESS

Previous studies have shown that compounding reactive blends based on nylon *x*, *y*-type materials in an appropriate twin-screw extruder, rather than the current single-screw extruder, can reduce the complexity and size of the rubber particles.[4] This has been attributed to the higher mixing intensity available in corotating twin-screw extruders. On this basis, the reactive systems described earlier for single-screw extrusion should have an increased probability of reaction and improved dispersion resulting in a finer morphology.

The Baker-Perkins twin-screw extruder used in this study was operated at 280°C and 175 rpm. It was necessary to operate the twin-screw extruder at higher temperatures than the single-screw extruder (280 vs. 240°C) and to restrict the maleation content of the rubber phase to 1% or less to lower melt viscosity in order not to exceed the torque limit of the small twin-screw extruder. For blends based on the amine-terminated nylon 6, XPN-1250, only the elastomers SEBS-*g*-MA-0.5% and SEBS-*g*-MA-1%

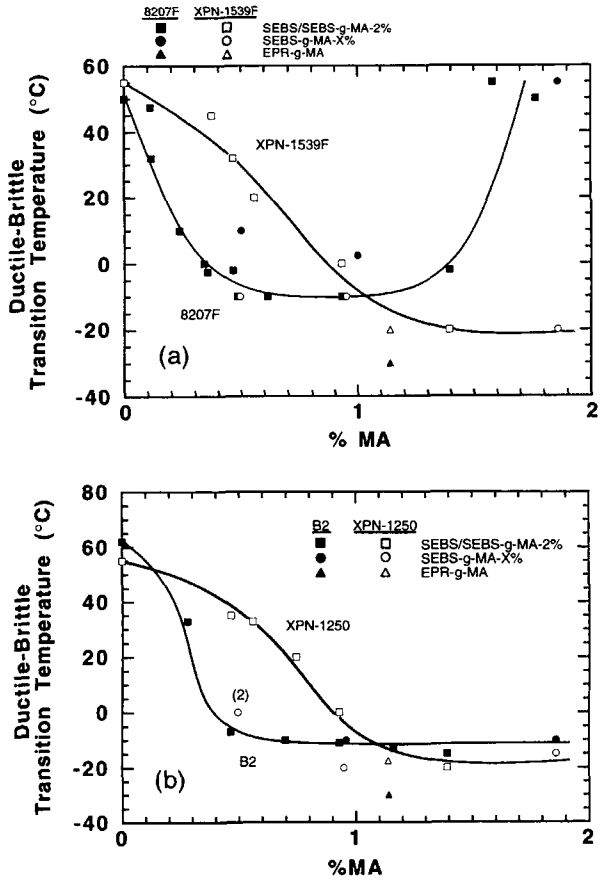

Figure 13 Effect of rubber-phase maleic anhydride content on the ductile–brittle transition temperature for blends of SEBS/SEBS-*g*-MA-2%, SEBS-*g*-MA-**X**%, and EPR-*g*-MA with difunctional and monofunctional polyamides in the ratio of 20% rubber/80% polyamide: (a) XPN-1539F and Capron 8207F; (b) XPN-1250 and B2.

were used. The copolyamide XPN-1539F and its monofunctional control were blended with the same two SEBS-*g*-MA-**X** % elastomers and EPR-*g*-MA. Blends of Capron 8207F were run under identical conditions as blends of XPN-1539F to determine whether changes in the morphology (or properties) were a result of either the higher processing temperature or the higher mixing intensity of the twin-screw extruder.

Tables III and IV show the results for blends with XPN-1539F and XPN-1250 compounded in the single- vs. the twin-screw extruder. There is a significant reduction in the rubber particle size and narrowing of the size distribution when the twin-screw extruder is used, whereas the mechanical properties[8] and toughness are essentially the same regardless of extruder type. Figure 15 shows TEM photomicrographs which compare the morphology of blends based on the two SEBS-*g*-MA-**X** % elastomers with the difunctional polyamides when compounded in the single- and twin-screw extruders. Clearly, the twin-screw extruder reduces the complexity and size of the rubber particles for these blends. Figure 16(a) shows that the Izod impact strength vs. the temperature relationship for blends with XPN-1250 are not affected by the extruder type. A reduction in the ductile–brittle transition temperature for blends of the amine-terminated nylon 6 with either of the SEBS-*g*-MA-**X** % elastomers was not expected since the values attained by the blends generated in the single-screw extruder are already at the limits for these materials.[49] However, reducing the rubber particle size for the blend of SEBS-*g*-MA-1% with XPN-1539F resulted in a 10°C reduction in the ductile–brittle transition

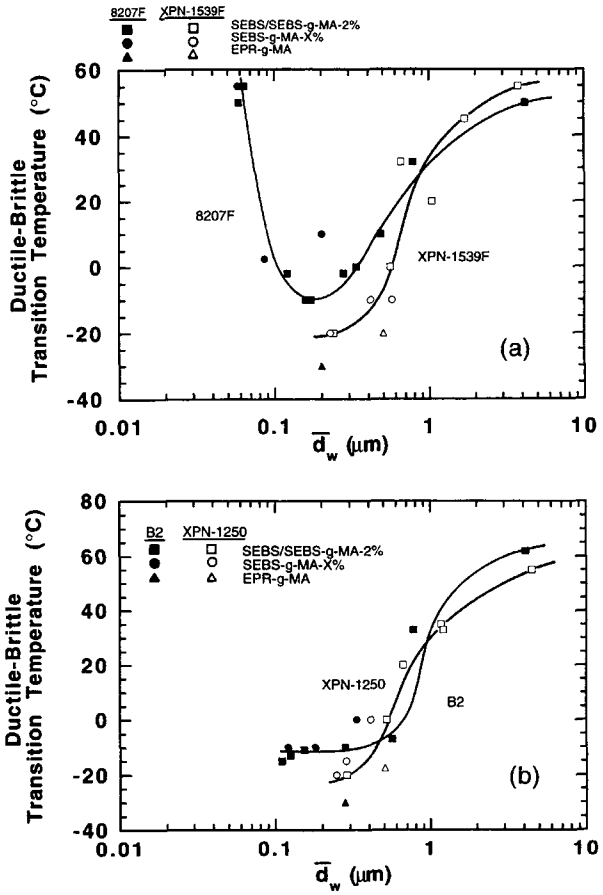

Figure 14 Effect of weight-average rubber particle diameter on the ductile–brittle transition temperature for blends of SEBS/SEBS-*g*-MA-2%, SEBS-*g*-MA-**X**%, and EPR-*g*-MA with difunctional and monofunctional polyamides in the ratio of 20% rubber/80% polyamide: (a) XPN-1539F and Capron 8207F; (b) XPN-1250 and B2.

Table III Characteristics of Blends Based on XPN-1250 Compounded in Single- and Twin-screw Extruders

	SEBS-*g*-MA-0.5%		SEBS-*g*-MA-1%	
	Single	Twin	Single	Twin
$\bar{d}_n$ (μm)	0.25	0.23	0.20	0.09
$\bar{d}_w$ (μm)	0.41	0.29	0.25	0.11
$\bar{d}_v$ (μm)	1.61	0.40	0.37	0.14
$\bar{d}_w/\bar{d}_n$	1.68	1.23	1.24	1.16
$\bar{d}_v/\bar{d}_n$	6.53	1.71	1.87	1.54
Izod impact (J/m)[a]	907	1065	1355	1370
Ductile–brittle transition temperature (°C)	0	−5	−20	−20

[a] Values at 24°C.

temperature as seen in Figure 16(b). No significant changes in either the rubber particle size or toughness is observed for the similar blends with Capron 8207F.

For the blends based on EPR-*g*-MA with XPN-1539F and Capron 8207F, the shape of the rubber phase is complex and contains occluded matrix material, regardless of extruder type.[8] When blended

Table IV Comparison of Blends Based on XPN-1539F and 8207F Compounded in Single- and Twin-Screw Extruders

Nylon	Extruder Type	$\bar{d}_n$ (μm)	$\bar{d}_w$ (μm)	$\bar{d}_v$ (μm)	$\bar{d}_w/\bar{d}_n$	$\bar{d}_v/\bar{d}_n$	Izod[c] (J/m)	Ductile–brittle transition temperature (°C)
20% SEBS-*g*-MA-0.5%/80% nylon								
XPN-1539F	Single[a]	0.39	0.57	0.98	1.48	2.53	1130	−10
XPN-1539F	Twin[b]	0.25	0.32	0.45	1.25	1.80	1132	−10
8207F	Twin[b]	0.22	0.28	0.43	1.26	1.95	739	−5
8207F	Single[a]	0.17	0.20	0.25	1.18	1.47	579	5
20% SEBS-*g*-MA-1%/80% nylon								
XPN-1539F	Single[a]	0.28	0.41	0.81	1.48	2.89	1359	−10
XPN-1539F	Twin[b]	0.14	0.20	0.34	1.36	2.35	1225	−20
8207F	Twin[b]	0.08	0.09	0.10	1.08	1.25	410	−10
8207F	Single[a]	0.08	0.09	0.1	1.05	1.17	357	0
20% EPR-*g*-MA/80% nylon								
XPN-1539F	Single[a]	0.35	0.50	1.07	1.43	3.03	1130	−20
XPN-1539F	Twin[b]	0.20	0.26	0.42	1.3	2.09	1124	−35
8207F	Twin[b]	0.29	0.26	0.46	1.36	2.39	583	−40
8207F	Single[a]	0.17	0.20	0.28	1.18	1.65	524	−35

[a] Processed at 240°C.
[b] Processed at 280°C.
[c] Value at 24°C.

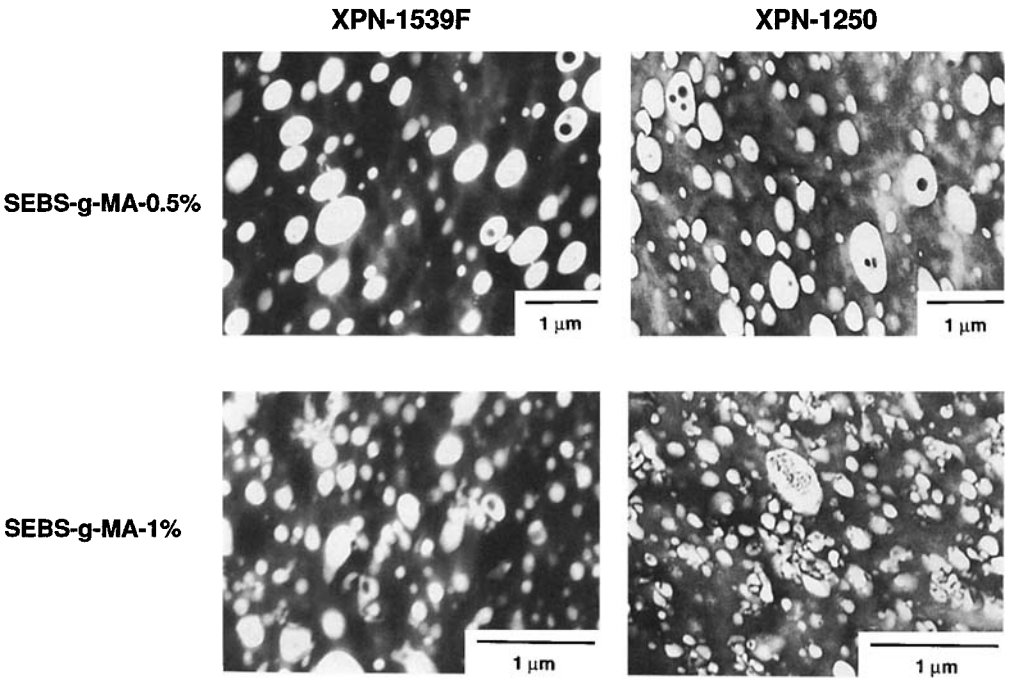

Figure 15 TEM photomicrographs of 20% SEBS-*g*-MA-**X**%/80% polyamide blends for **X** = 0.5 and 1% MA when compounded in a twin-screw extruder with the difunctional polyamides XPN-1539F and XPN-1250. The polyamide phase is stained dark with phosphotungstic acid.

in the twin-screw extruder, the rubber particle size is reduced by a factor of two for the XPN-1539F blend which decreases the ductile–brittle transition temperature of the blend from −20 to −35°C (see Fig. 17). Based on previous studies,[8,49] a similar reduction in the ductile–brittle transition temperature would be expected for the blend of EPR-*g*-MA with XPN-1250 if the particle size could be reduced by blending in the twin-screw extruder. The toughness of the blend based on Capron 8207F did not change since the rubber particle size produced in the twin-screw extruder was the same as that from the single-screw extruder.

From the above results, it can be concluded that the higher processing temperatures and mixing intensity has little affect on the rubber particle size or mechanical properties for blends with Capron 8207F, but, evidently, the higher mixing intensity produced in the twin-screw extruder is needed to reduce the rubber particle size and distribution for blends of XPN-1250 and XPN-1539F with maleated elastomers.

CONCLUSIONS

This study of the effects of polyamide end-group configuration and the maleic anhydride content of the rubber on blend morphology and mechanical properties has led to the following conclusions: In a single-screw extruder, blends with the two difunctional polyamides, a copolyamide containing 15% nylon 6,6 and an amine-terminated nylon 6, produce rubber particles that are larger, more complex, and contain occluded matrix material, whereas blends based on the monofunctional nylon 6 control materials of equivalent melt viscosity have very small, spherical elastomeric particles. This difference in morphology was attributed to the crosslinking-type effects from the fraction of chains with two amine end groups that can react with the maleic anhydride in the rubber phase. Analysis of amine group content before and after blending revealed that a greater number of amine groups react with EPR-*g*-MA and SEBS-*g*-MA-2% elastomers in the case of the difunctional polyamides than for blends with the monofunctional nylon 6 materials. Torque rheometry revealed that blends with the difunctional polyamides produce higher melt viscosities than do similar blends with the monofunctional controls due to the crosslinking-type graft reactions.

Blends based on the difunctional polyamides have higher room-temperature Izod impact strength than those for the corresponding control materials;

however, subambient toughness depends mainly on the inherent ductility of the matrix material. The copolyamide, XPN-1539F, has a lower degree of crystallinity and tensile modulus than does its monofunctional control, which is believed to cause blends with the former to have lower ductile–brittle transition temperatures at the same rubber particle size than do blends with the latter.

Use of a twin-screw extruder was used to reduce the size and complexity of the rubber phase for blends with the difunctional polyamides. The reduction in rubber particle size for blends with the copolyamide resulted in lower ductile–brittle transition temperatures. Blends based on the monofunctional control for the copolyamide showed no appreciable differences in morphology or toughness when compounded in the single- vs. twin-screw extruders.

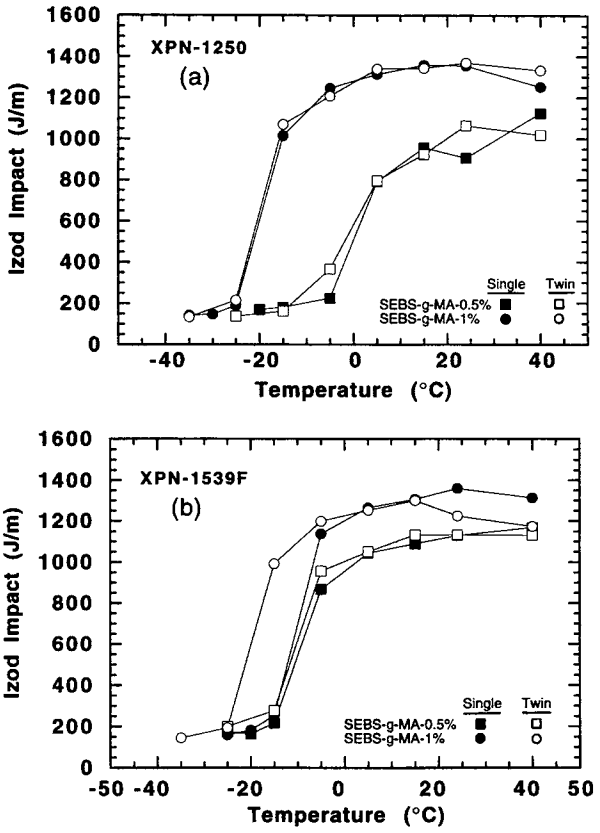

Figure 16 Effect of extruder type on Izod impact strength vs. temperature for blends of 20% SEBS-*g*-MA-X%/80% difunctional polyamide for **X** = 0.5 and 1% with the following polyamides: (a) XPN-1250; (b) XPN-1539F.

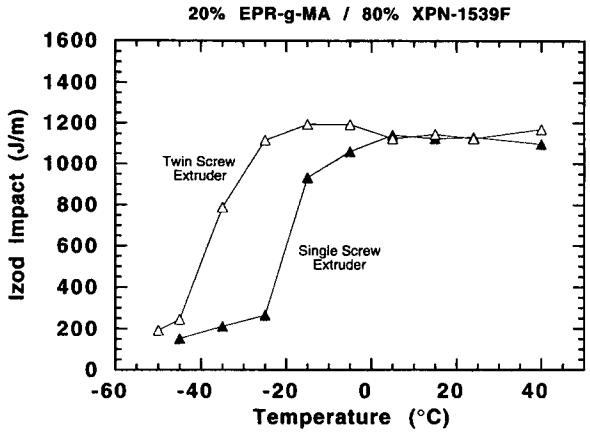

Figure 17 Effect of extruder type on Izod impact strength vs. temperature for 20% EPR-*g*-MA/80% difunctional polyamide (XPN-1539F) blends.

This work was supported by the U.S. Army Research Office. The authors would like to thank Allied-Signal Inc., BASF Corp., Exxon Chemical Co., and Shell Development Co. for the materials and technical communications. The authors would also like to thank Dr. Biswaroop Majumdar for his contributions in the area of transmission electron microscopy.

REFERENCES

1. A. J. Oshinski, H. Keskkula, and D. R. Paul, *Polymer*, **33**, 284 (1992).
2. Y. Takeda, H. Keskkula, and D. R. Paul, *Polymer*, **33**, 3173 (1992).
3. B. Majumdar, H. Keskkula, and D. R. Paul, *Polymer*, **35**, 5468 (1994).
4. B. Majumdar, H. Keskkula, and D. R. Paul, *J. Appl. Polym. Sci.*, **54**, 339 (1994).
5. A. J. Oshinski, H. Keskkula, and D. R. Paul, *Polymer*, **33**, 268 (1992).
6. C. D. Mason, U.S. Pat. 4,945,129 (1990) (to Allied-Signal Inc.).
7. Y. Takeda, University of Texas at Austin, personal communication, 1991.
8. A. J. Oshinski, PhD Dissertation, University of Texas at Austin, 1995.
9. L. Schlanger, Allied-Signal, Inc., personal communication, 1995.
10. P. Gilmore, Allied-Signal, Inc., personnal communication, 1993.
11. A. Ilg, BASF Corp., personnal communication, 1993.
12. D. Hansen, Shell Development Co., personal communication, 1993.
13. G. Bach, in *Quantitative Methods in Morphology*, E. R. Weibel and M. Elias, Eds., Springer-Verlag, Berlin, 1967.

14. R. R. Irani and C. F. Callis, *Particle Size: Measurement, Interpretation and Application,* Wiley, New York, 1963.
15. E. M. Chamot and C. W. Mason, *Handbook of Chemical Microscopy,* Wiley, London, 1983.
16. R. J. M. Borggreve, R. J. Gaymans, J. Schuijer, and J. F. Ingen Housz, *Polymer,* **28,** 1489 (1987).
17. B. D. Favis, *Can. J. Chem. Eng.,* **69,** 619 (1991).
18. K. Dijkstra, PhD Dissertation, University of Twente, 1993.
19. M. I. Kohan, *Nylon Plastics,* Wiley, New York, 1977.
20. J. Urbanski, W. Czerwinski, K. Janicka, F. Majewska, and H. Zowall, in *Handbook of Analysis of Synthetic Polymers and Plastics,* Wiley, New York, 1972.
21. Allied-Signal Inc., *Analytical Sciences at Allied-Signal,* internal publication, 1988, p. 93.
22. H. K. Reimschuessel and G. J. Dege, *J. Polym. Sci. Part A-1,* **9,** 2342 (1971).
23. J. Zimmerman, *Encyclopedia of Polymer Science and Engineering,* 2nd ed., Wiley-Interscience, New York, 1988, Vol. 11, p. 353.
24. R. E. Putscher, *Kirk-Othmer Encyclopedia of Chemical Technology,* 3rd ed., Wiley-Interscience, New York, 1982, Vol. 18, p. 328.
25. J. J. Burke and T. A. Orofino, *J. Polym. Sci. Part A-2,* **7,** 1 (1969).
26. J. E. Waltz and G. B. Taylor, *Anal. Chem.,* **19,** 448 (1947).
27. P. Marechal, G. Coppens, R. Legras, and J. M. Dekoninck, *J. Polym. Sci. Part A Polym. Chem.,* **33,** 757 (1995).
28. D. F. Lawson, W. L. Hergenrother, and M. G. Matlock, *J. Appl. Polym. Sci.,* **39,** 2331 (1990).
29. Z. Tuzar and P. J. Kratochvil, *J. Polym. Sci. Polym. Lett. Ed.,* **3,** 17 (1965).
30. A. J. Oshinski, H. Keskkula, and D. R. Paul, to appear.
31. G. M. Jordhamo, J. A. Manson, and L. H. Sperling, *Polym. Eng. Sci.,* **26,** 517 (1986).
32. B. D. Favis and J. P. Chalifoux, *Polym. Eng. Sci.,* **27,** 1591 (1987).
33. B. D. Favis and J. M. Willis, *J. Polym. Sci. B,* **28,** 2259 (1990).
34. B. D. Favis, J. P. Chalifoux, and P. Van Gheluwe, *Soc. Plast. Eng. ANTEC,* **45,** 169 (1987).
35. G. Serpe, J. Jarrin, and F. Dawans, *Polym. Eng. Sci.,* **30,** 553 (1990).
36. S. S. Dagli, M. Xanthos, and J. A. Biesenberger, in *Compalloy 1991, Proceedings of the Fourth International Congress on Compatibilizers and Reactive Polymer Alloying,* New Orleans, LA, 1991, p. 257.
37. G. I. Taylor, *Proc. R. Soc. (Lond.) A,* **146,** 501 (1934).
38. H. P. Grace, *Chem. Eng. Commun.,* **14,** 225 (1982).
39. S. Wu, *Polym. Eng. Sci.,* **27,** 335 (1987).
40. M. W. Fowler and W. E. Baker, *Polym. Eng. Sci.,* **28,** 21 (1988).
41. R. E. Baker and M. Saleem, *Polymer,* **28,** 2057 (1987).
42. V. J. Triacca, S. Ziaee, J. W. Barlow, H. Keskkula, and D. R. Paul, *Polymer,* **32,** 1401 (1991).
43. J. W. Barlow, G. P. Shaver, and D. R. Paul, in *Proceedings of First International Congress on Compatibilizers and Reactive Polymer Alloying (Compalloy '89),* New Orleans, LA, 1989, p. 221.
44. A. E. Flexman, *Polym. Eng. Sci.,* **19,** 564 (1979).
45. S. Wu, *Polymer,* **26,** 1855 (1985).
46. S. Y. Hobbs, R. C. Bopp, and V. H. Watkins, *Polym. Eng. Sci.,* **23,** 380 (1983).
47. A. J. Oostenbrink, L. J. Molenaar, and R. J. Gaymans, Poster given at *6th Annual Meeting of Polymer Processing Society,* Nice, France, April 18–20, 1990.
48. A. J. Oshinski, H. Keskkula, and D. R. Paul, to appear.
49. A. J. Oshinski, H. Keskkula, and D. R. Paul, to appear.
50. J. N. Goodier, *Trans. Am. Soc. Mech. Eng.,* **55,** 39 (1933).
51. R. J. Oxborough and P. B. Bowden, *Philos. Mag.,* **30,** 171 (1974).
52. C. B. Bucknall and A. J. Lazzeri, *J. Mater. Sci.,* **28,** 6799 (1993).
53. B. N. Epstein, U.S. Pat. 4,174,358 (1979) (to E. I. DuPont Co.).
54. B. N. Epstein, U.S. Pat. 4,172,859 (1979) (to E. I. DuPont Co.).
55. O. K. Muratoglu, A. S. Argon, and R. E. Cohen, *Polymer,* **36,** 921 (1995).

Received September 28, 1995
Accepted January 23, 1996